Crystalline Ordering in Silica and Germania Glasses

Abstract. *The diffraction patterns of both silica and germania glasses are consistent with a structure in which nearly all of the atoms belong to tridymite-like regions of up to about 20 angstroms or more that are bonded efficiently together in a manner analogous to that found in twinned crystals.*

Two limiting models have been proposed for glasses. In one model (*1*) the material is depicted as composed of small regions of crystalline-like order bonded together in essentially random orientations; in the other model the glass structure is described as a random network (*2*) in which the distribution of only the shortest interatomic distances corresponds throughout the material to those present in a crystalline phase. Diffraction analyses performed on silica glass (*3, 4*) and germania glass (*4, 5*) have been generally interpreted in terms of the random network model.

Recently Leadbetter and Wright (*6*) reported an x-ray diffraction study on germania glass in which a quartz-like structure was assigned to the interatomic distances ranging out to 10.5 Å. In another recent investigation, Konnert and Karle (*7*) found the x-ray diffraction pattern of silica glass to be consistent with a structure composed nearly entirely of ordered regions similar to those of the crystalline polymorph tridymite having dimensions up to at least 13 Å. In this report we describe further refinements of the x-ray diffraction data and additional evidence from neutron diffraction data in support of a tridymite-like structure for both the silica and germania glasses.

We collected x-ray diffraction data with Mo$K\alpha$ radiation, using fused quartz and fused silica from the vapor-phase hydrolysis of pure silicon compounds (Infrasil and Suprasil, respectively, prepared by Amersil, Inc.). All data sets produced nearly identical radial distribution functions (RDF's). We collected neutron diffraction data at a wavelength of 0.84 Å at the National Bureau of Standards, using Suprasil and germania glass samples prepared at the Naval Research Laboratory by R. Ginther. The RDF's are illustrated in Fig. 1. Significant deviations from a uniform distribution of distances are present out to at least 20 Å.

Full details of the data reduction will be published elsewhere (*8*). However, since this procedure has revealed previously undetected details in the RDF's, the main points of the procedure will be mentioned. The basic considerations concern the imposition of constraints on the RDF (*9*). That portion of the total intensity function that contains interatomic distance information, $i(s)$, is isolated in a manner described for electron diffraction (*10*). We handled the truncation problem by recognizing that in the usual experiments only the shortest distances are sufficiently ordered to contribute to $i(s)$ beyond the experimental limit of data collection. These short distance (SD) contributions are removed from $i(s)$ by a least-squares procedure that minimizes the spurious detail in the RDF at small and large values of r. The equation employed is:

$$r^2D(r) = 4\pi r^2[\rho(r) - \rho_0] = \frac{2\pi}{r}\int_0^{s_{\max}} s[Ki(s) - \sum_{\mathrm{SD}} \frac{N_{ij}f_if_j \exp(-\ell^2_{ij}s^2/2)}{sr_{ij}\sum_{\mathrm{UC}} f^2} \sin sr_{ij}] \sin sr\, ds + \text{SD contributions}$$

where $s = (4\pi \sin\theta)/\lambda$, λ is the wavelength, 2θ is the angle between the incident and diffracted beam, K places the intensity on an absolute scale, r_{ij} is the distance between the ith and jth atoms, N_{ij} is the coordination number, ℓ_{ij} is the disorder parameter, UC is the unit of composition (SiO_2 or GeO_2), $s_{\max}$ is the experimental limit of data collection, the f's are the atomic scattering factors, ρ_0 is the density parameter, and $4\pi r^2\rho(r)$ is the probability weighted by the scattering factors of finding atoms in the sample separated by the distance r. The short distances are reintroduced without associated truncation effects into the final RDF.

The densities of the polymorphs of silica (in grams per cubic centimeter: 2.20 for the silica glass, 2.31 for tridymite, 2.32 for cristobalite, 2.49 for keatite, 2.65 for quartz, 3.01 for coesite, and 4.28 for stishovite) suggest that the structures of tridymite and cristobalite might be related to the predominant atomic arrangements in this glass. Crystalline germania is known to exist in two basic modifications: a quartz-type structure with a density of 4.2 g/cm^3 and a rutile structure with a density of 6.2 g/cm^3. The density of germania glass is only 3.65 g/cm^3. Significant, however, is the fact that the ratio of the densities of germania glass to quartz-like germania is precisely the same as the ratio of the densities of tridymite to quartz.

We calculated RDF's for the crystalline forms by broadening the Bragg maxima in the powder patterns to correspond to an 11-Å particle size for three quarters of the sample and a 20-Å size for one quarter. Such broadening reduces the amplitudes of the RDF without altering the positions of the peaks, thus affording a suitable approximation to the RDF corresponding to small ordered regions. If the dimensions of these regions are less than the unit cell dimensions, the result is that all configurations in the unit cell are represented by different particles.

Atomic parameters obtained from crystal structure analyses were used to calculate the diffraction patterns for quartz (*11*) and cristobalite (*12*). Since tridymite forms highly twinned crystals with a variety of unit cells (all with a subcell of approximate dimensions $a = 8.6$ Å, $b = 5.0$ Å, $c = 8.2$ Å), accurate atomic parameters are not available. The average structure has been determined at 250°C and provides evidence for the bonding topology (*13*).

A powder diffraction pattern collected for a sample of tridymite from Diamond Lake, Douglas County, Oregon, showed orthorhombic diffraction symmetry with $a = 81.97$ Å, $b = 9.94$ Å, and $c = 17.23$ Å. The approximate percentages (by weight) of impurities, as indicated by electron probe analysis, are as follows: Al, ~ 2 percent; Na, ~ 1 percent; and K, ~ 1 percent. Accurate atomic positions have not been determined for the crystalline polymorphs of germania. The neutron powder diffraction patterns for quartz-like and cristobalite-like germania were calculated with the use of the atomic coordinates of quartz and cristobalite and the appropriate scattering factors for neutrons.

The $r^3D(r)$ curves are illustrated in Fig. 1. The x-ray RDF for silica glass is quite similar to the RDF derived from the powdered tridymite but quite different from the RDF's derived from cristobalite and quartz. The positions of the maxima in the silica glass RDF's obtained from neutron and x-ray diffraction data are nearly the same, an indication that the distances tend to cluster similarly. The germania glass RDF obtained from the neutron diffraction data is very similar to the silica glass RDF obtained from the x-ray data. The Ge and O atoms scatter neutrons with approximately the same relative efficiency as Si and O atoms scatter x-rays, as illustrated by the similarity of the neutron diffraction RDF's calculated for quartz-like and cristobalite-like germania to the x-ray RDF's of quartz and cristobalite. Thus the RDF's strongly suggest that silica glass, germania glass, and tridymite possess the same short-range order.

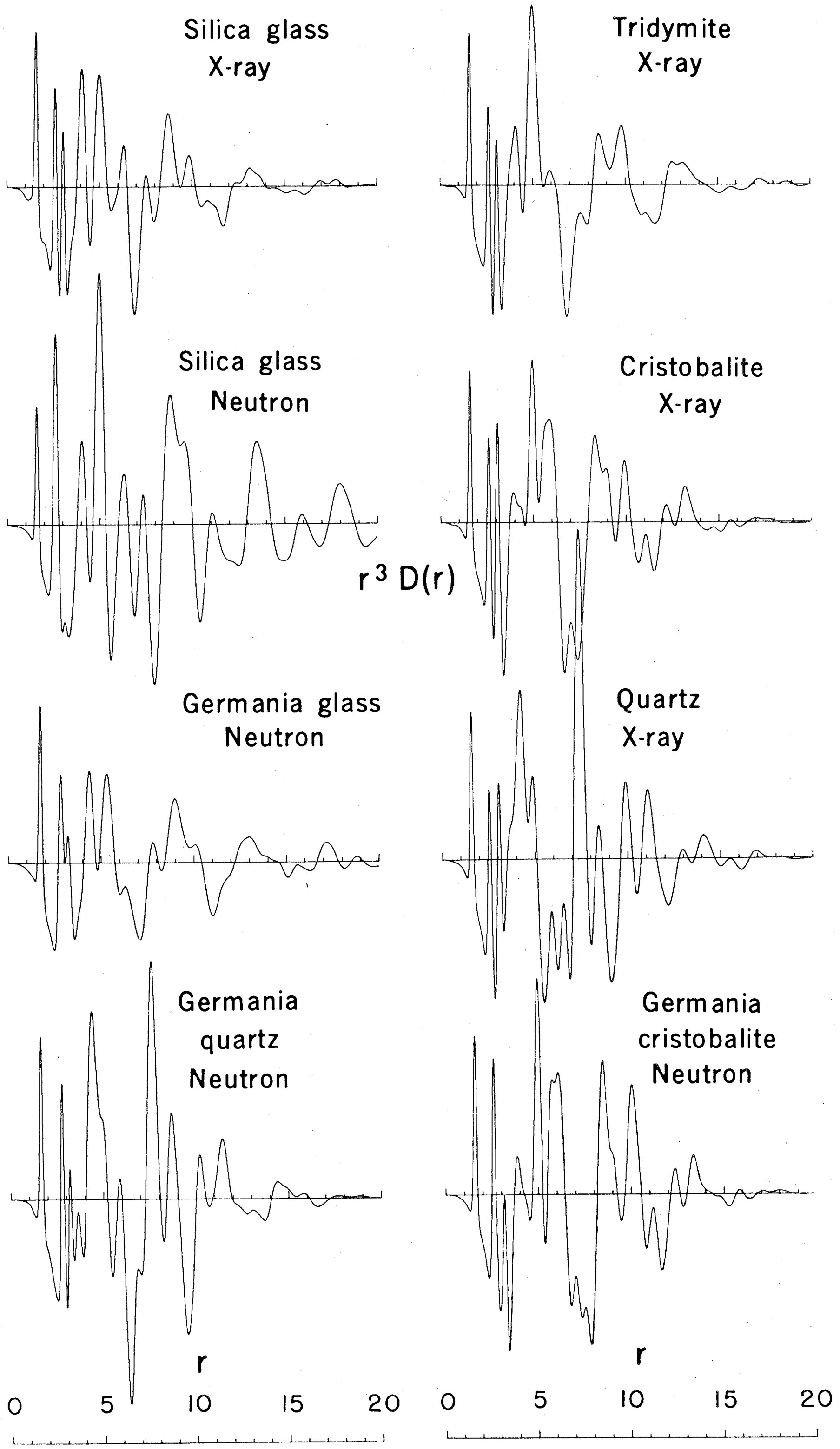

Fig. 1. Radial distribution functions [$r^3D(r)$] for silica and germania glasses and comparison functions derived from the broadened powder patterns of crystalline polymorphs.

The correspondence of the positions and magnitudes of the details in the RDF's obtained for silica glass and tridymite-like particles indicates that the data are consistent with a structure in which nearly all of the atoms comprise parts of tridymite-like regions having dimensions ranging up to at least 20 Å. Details at large *r* suggest the possibility of a small amount of cristobalite-like ordering. The relatively large details in the outer portion of the RDF for silica glass from the neutron diffraction data may arise from the O atoms, the dominant neutron scatterers, lying on the periphery of the ordered regions. However, the larger sample used for the neutron diffraction experiment may, in fact, be more highly ordered.

If the interpretation that nearly all atoms are part of ordered regions is correct, it is necessary that these regions be efficiently bonded together in a manner analogous to that found in twinned crystals, but with a fairly large number of relative orientations and small distortions so that isotropic properties would be present. Differences in the inner regions of the RDF's of silica glass and tridymite computed from the x-ray diffraction data can be related to the junctures between the ordered regions. The three shortest distances throughout the glass samples are nearly identical to the corresponding distances in all of the crystalline modifications where the silicon atoms are tetrahedrally bonded. The contribution to the RDF from distances between atoms in different ordered regions would be progressively less as *r* increases, and beyond about 6 Å they would not contribute any appreciable details.

Although radial distribution functions of glasses do not alone provide enough information for a unique structure determination, the comparisons with the functions calculated from crystalline phases of nearly the same density as the glasses imply a great similarity between glasses and crystals on the atomic level.

J. H. KONNERT
J. KARLE
Laboratory for the Structure of Matter, Naval Research Laboratory, Washington, D.C. 20390
G. A. FERGUSON
Naval Research Laboratory and *Howard University, Washington, D.C. 20001*

References and Notes

1. N. Valenkov and E. Porai-Koshits, *Z. Kristallogr.* **91**, 195 (1936).
2. W. H. Zachariasen, *J. Amer. Chem. Soc.* **54**, 3841 (1932).
3. C. Carraro, M. Domenici, T. Zucca, in *Physics of Non-Crystalline Solids*, J. A. Prins, Ed. (North-Holland, Amsterdam, 1965), pp. 152–161; E. H. Henninger, R. C. Buschert, L. Heaten, *J. Phys. Chem. Solids* **28**, 423 (1967); R. L. Mozzi and B. E. Warren, *J. Appl. Crystallogr.* **2**, 164 (1969); R. L. Mozzi, thesis, Massachusetts Institute of Technology (1967).
4. E. Lorch, *Proc. Phys. Soc. London Solid State Phys.* **2**, 229 (1969).
5. G. A. Ferguson and M. Hass, *J. Amer. Ceram. Soc.* **53**, 109 (1970).
6. A. J. Leadbetter and A. C. Wright, *J. Non-Cryst. Solids* **7**, 37 (1972).
7. J. H. Konnert and J. Karle, *Nature Phys. Sci.* **236**, 92 (1972).
8. ———, in preparation.
9. I. L. Karle and J. Karle, *J. Chem. Phys.* **17**, 1052 (1949); *ibid.* **18**, 957 (1950); *ibid.*, p. 963.
10. P. D'Antonio, C. George, A. H. Lowrey, J. Karle, *J. Chem. Phys.* **55**, 1071 (1971).
11. R. A. Young and B. Post, *Acta Crystallogr.* **15**, 337 (1962).
12. W. A. Dollase, *Z. Kristallogr.* **121**, 369 (1965).
13. ———, *Acta Crystallogr.* **23**, 617 (1967).
14. We thank L. Paollela for his aid in collecting the neutron diffraction data. The research was supported in part by the Advanced Research Projects Agency.

19 May 1972

High-Resolution Spectroscopy of the Earth's Free Oscillations, Knowing the Earthquake Source Mechanism

Abstract. *A new method for identification of normal modes of oscillation of the earth yielded unambiguous determinations of many overtones never before identified. This method consists of the superposition of spectra observed at many stations over the earth, after a correction for the phase determined from the known earthquake source mechanism.*

After a large earthquake, such as the Alaskan earthquake of 28 March 1964, the earth continues to vibrate for days or even weeks. These vibrations consist of a superposition of the infinite number of normal modes of oscillation of the earth; the determination of the eigenfrequency corresponding to each mode is of great importance in revealing the properties of the earth's interior. Each mode manifests itself as a sharp peak in the ground displacement spectrum as observed at a seismological station. The identification of a peak in such a spectrum as corresponding to a given mode is relatively simple for the low-frequency range, where only the lower overtones exist and the peaks are well separated from each other. The usual method of identifying a peak consists of matching theoretical to observed eigenfrequencies, complemented by some additional criteria (*1*). For higher frequencies the separation between peaks becomes smaller, and in general for periods below 250 seconds the peaks can not be unambiguously identified by the usual methods.

Here I report a new method of identification, the excitation criterion. It requires a knowledge of the source mechanism of the earthquake exciting the free oscillations, and it is necessary to have observations from many seismographs all over the earth. The method consists of the following steps. First the theoretical amplitude and phase are computed at all the observing stations for the mode to be identified, say, the mode ${}_5S_{26}$, as excited by a double couple model of the earthquake, with its geometry determined from the first motion of *P* waves, in a realistic spherically symmetric model of the earth (*2*). I assumed a step function as source time function. For wavelengths much longer than the dimensions of the earthquake fault the theoretical phase of a spectral peak can only be 0 or π (*3*). A factor of π is then added to the phase of the observed spectra at those stations where the theoretical phase of ${}_5S_{26}$ is π, leaving the spectra at all other stations unchanged. With this correction the phase of ${}_5S_{26}$ will be the same at all the observing stations, while for other modes the phase will be π at some stations and 0 at others. Finally, all the spectra are vectorially added. Through this summation the peaks of ${}_5S_{26}$ will add constructively because they have

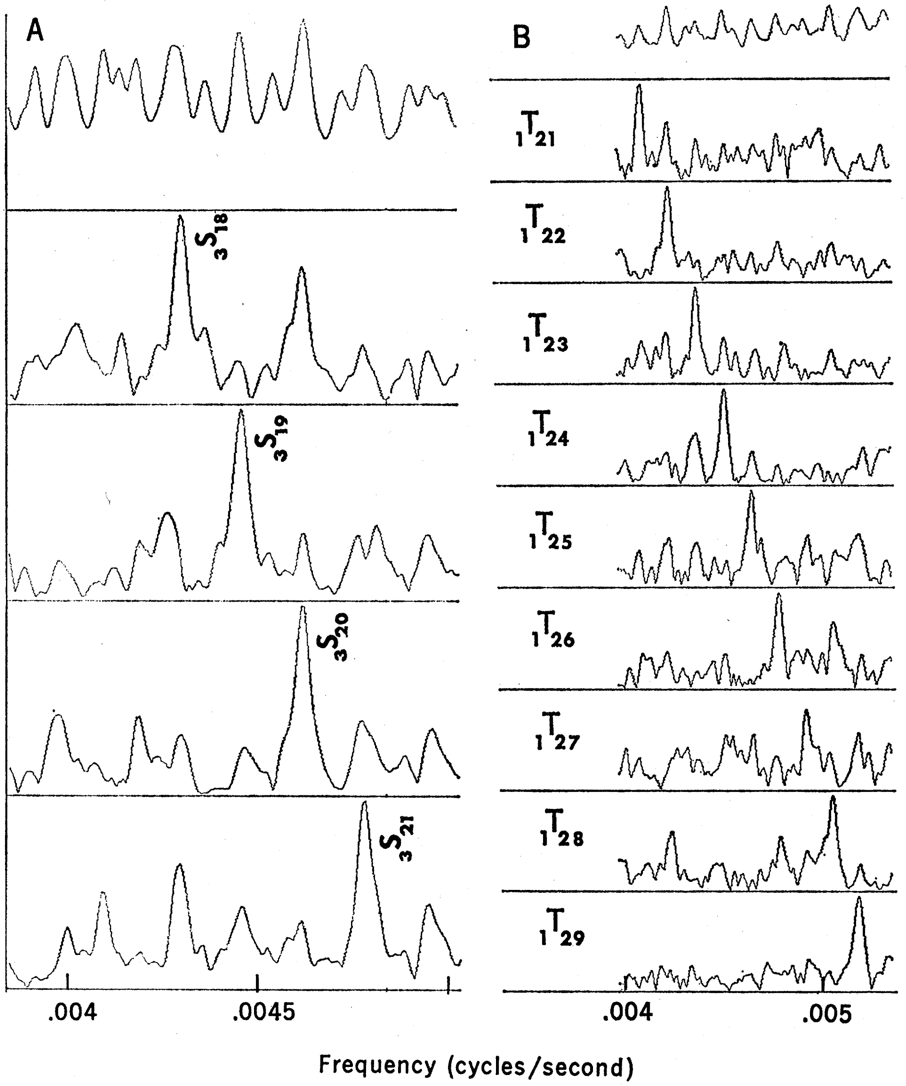

Fig. 1. Examples of identification of spectral peaks for the third higher spheroidal modes ${}_3S$ in the colatitudinal component (A), and the first higher torsional modes ${}_1T$ in the azimuthal component (B). The spectra at the top are the sums of the absolute amplitudes of the spectra at all the stations. The remaining spectra are the result of using the excitation criterion to identify spectral peaks.